Pediatric RESEARCH

www.nature.com/pr

BASIC SCIENCE ARTICLE

Developmental window of vulnerability to white matter injury driven by sublethal intermittent hypoxemia

Sergey A. Sosunov[1], Zoya V. Niatsetskaya[1], Anna A. Stepanova[1], Alexander S. Galkin[1], Courtney E. Juliano[2], Veniamin I. Ratner[2] and Vadim S. Ten[1]

BACKGROUND: In the developing brain, the death of immature oligodendrocytes (OLs) has been proposed to explain a developmental window for vulnerability to white matter injury (WMI). However, in neonatal mice, chronic sublethal intermittent hypoxia (IH) recapitulates the phenotype of diffuse WMI without affecting cellular viability. This work determines whether, in neonatal mice, a developmental window of WMI vulnerability exists in the absence of OLs lineage cellular death.
METHODS: Neonatal mice were exposed to cell-nonlethal early or late IH stress. The presence or absence of WMI phenotype in their adulthood was defined by the extent of sensorimotor deficit and diffuse cerebral hypomyelination. A separate cohort of mice was examined for markers of cellular degeneration and OLs maturation.
RESULTS: Compared to normoxic littermates, only mice exposed to early IH stress demonstrated arrested OLs maturation, diffuse cerebral hypomyelination, and sensorimotor deficit. No cellular death associated with IH was detected.
CONCLUSIONS: Neonatal sublethal IH recapitulates the phenotype of diffuse WMI only when IH stress coincides with the developmental stage of primary white matter myelination. This signifies a contribution of cell-nonlethal mechanisms in defining the developmental window of vulnerability to diffuse WMI.

Pediatric Research _####################_; https://doi.org/10.1038/s41390-021-01555-x

IMPACT:

- The key message of our work is that the developmental window of vulnerability to the WMI driven by intermittent hypoxemia exists even in the absence of excessive OLs and other cells death.
- This is an important finding because the existence of the developmental window of vulnerability to WMI has been explained by a lethal-selective sensitivity of immature OLs to hypoxic and ischemic stress, which coincided with their differentiation.
- Thus, our study expands mechanistic explanation of a developmental window of sensitivity to WMI by showing the existence of cell-nonlethal pathways responsible for this biological phenomenon.

INTRODUCTION

Clinical advances in neonatal intensive care have improved the survival of very low birth weight and extremely low birth weight infants. However, these survival gains come with increased risk for certain complications associated with preterm birth. White matter injury (WMI) and associated neurologic disability represent significant morbidities and have increased in incidence with the survival of smaller and sicker premature infants.[1] The neuropathological spectrum of WMI ranges from extensive white matter loss defined as cystic periventricular leukomalacia (PVL) to focal microscopic gliosis and diffuse cerebral hypomyelination.[2] Recently, non-cystic diffuse WMI has become a predominant neuropathological lesion in premature infants with brain injury.[2,3] Preterm birth is the primary risk factor for the development of WMI, with delivery at 23–29 weeks conferring the highest risk. This gestational age corresponds to the onset and initiation of primary myelination in the developing brain.[4,5] It has been proposed that excessive and selective death of oligodendrocyte precursors (OPCs) and immature pre-oligodendrocytes (pre-OLs) prior to primary myelination disrupts oligodendrocyte (OL) maturation, leading to cerebral myelination failure.[6] This hypothesis implies that a lethal cellular insult (i.e., an oxidative stress or ischemia) results in permanent depletion of pre-myelinating and myelinating OLs, leading to global cerebral hypomyelination.

Recently, we have reported a mouse model of neonatal chronic intermittent hypoxia (IH) stress, in which diffuse cerebral hypomyelination and sensorimotor neurological deficit were reproduced in the absence of excessive cellular death in the brain.[7,8] The fact that the phenotype of diffuse WMI can be replicated in the absence of OPCs and pre-OLs degeneration[8] suggests that the death/loss of immature OLs prior to and during active primary myelination is not an exclusive mechanism of the developmental window of vulnerability to WMI.

Sublethal chronic IH stress is one of the most common clinical manifestations of prematurity.[9] In extremely premature infants, IH stress has been associated with a significantly increased

[1]Department of Pediatrics, Division of Neonatology, Columbia University, New York, NY, USA; [2]Department of Pediatrics, Division of Neonatology, Icahn Mount Sinai School of Medicine, New York, NY, USA
Correspondence: Vadim S. Ten (vt82@cumc.columbia.edu)

Received: 1 December 2020 Revised: 9 April 2021 Accepted: 12 April 2021
Published online: 04 May 2021

probability of neurodevelopmental impairment or late death.[9] It has also been reported that, in human infants, the frequency of daily IH events peaks during the initial 6–8 weeks, following a premature birth.[10] This time frame coincides with the period of the most active OL differentiation.

This study was undertaken to determine if there is a critical time interval (developmental window), when the brain is highly vulnerable to IH that causes WMI. We have shown that IH during the first 10 days of life results in diffuse WMI due to arrested OL/s differentiation, without cellular death in the brain.

METHODS

The model of diffuse WMI and experimental design

All experiments were approved by the Columbia University Institutional Animal Care and Use Committee in accordance with AAALAC guidelines. The murine model of IH-induced WMI has been described previously.[7] Briefly, C57BL/6J newborn mice were exposed to 30 IH events daily. Each hypoxic event consisted of 3 min of exposure to 8% O_2, followed by 5 min of reoxygenation in room air at the ambient temperature of 34 °C. Experimental design and study groups are shown in Fig. 1a. There were two experimental groups: early exposure to IH (EIH) from postnatal day 1 (P1, day of birth was defined as P0) until P10 and late exposure to IH (LIH)—from P10 until P20. These ages for IH exposure were selected because primary white matter myelination in rodents peaks during the initial postnatal weeks,[11] and expression of genes coding myelin proteins reaches the maximum at P20.[12] Control groups consisted of littermates that were separated from their dams for the same period of time as their IH counterparts, but were kept in the normoxic environment at 34 °C. Following IH, mice were raised until their adulthood (P90). In adult mice, following neurofunctional assessment, an extent of cerebral myelination was examined with immunohistochemistry, western blotting for myelin basic protein (MBP) and 2′, 3′-cyclic-nucleotide 3′-phosphodiesterase (CNP-ase), and electron microscopy of the corpus callosum (CC) and external capsule (EC). Sex of mice was determined by abdominal exam upon euthanasia.

Sensorimotor phenotype in adult mice was evaluated using behavior tests. Normoxic animals used to control for effects in EIH or LIH groups at the age of P85–86 were combined into a single control group, as no difference in either cerebral myelination or sensorimotor performance has been detected. Upon completion of the neurofunctional assessment, P90 mice were euthanized for neuropathological and electron microscopy evaluation of their brains.

A separate cohort of control and experimental mice were euthanized at P1, P5, P10, P15, and P20 for immunohistochemical analysis of developmental myelination, maturation of the OL lineage cells, and for assessment of the extent of cell death in the brains.

Immunohistochemistry

The animals were euthanized by decapitation under deep isoflurane anesthesia. Brains were harvested, fixed in 4% paraformaldehyde (PFA) in 0.1 M phosphate buffer (PB) at 4 °C overnight. A total of 50 µm coronal sections were obtained using a vibratome (VT1000S, Leica Biosystems Inc., Buffalo Grove, IL), kept in cryoprotectant solution at −20 °C until usage. For immunofluorescence staining, after blocking with 10% goat serum for 30 min at room temperature (RT), free-floating sections were incubated with primary antibodies and secondary antibodies conjugated with fluorochromes (Alexa Fluor Antibodies, Life Technologies, CA) for 1 h at RT. DAPI was used for the visualization of the nuclei. Blocking solution, and primary and secondary antibodies were applied in 0.3% Triton in PBS. Sections were mounted on slides in Vectashield (Vector Laboratories, Burlingame, CA) and examined under confocal microscopy A1RMP+ (Nikon Instruments, Melville, NY).

For peroxidase immunostaining, free-floating sections were treated with 0.3% H_2O_2 in PBS (30 min, RT), blocked with 10% donkey serum, followed by incubation with primary antibody (anti-MBP) overnight at 4 °C. Secondary biotinylated antibody and Avidin–Biotin complex kit (Vector Laboratories, Burlingame, CA) were applied for 1 h at RT. Visualization with DAB (MilliporeSigma, St. Louis, MO) was performed, according to manufacture recommendations. Blocking solution, and primary and secondary antibodies were diluted in 0.3% Triton in PBS.

Primary antibodies included mouse monoclonal anti-APC (CC1; 1:400, #MABC200, MilliporeSigma, St. Louis, MO), rabbit polyclonal anti-NG2 (1:100, #AB5320, MilliporeSigma, St. Louis, MO), chicken polyclonal anti-MBP (1:400, #AB9348, MilliporeSigma, St. Louis, MO), rabbit polyclonal anti-cleaved caspase-3 (1:100, #9661, Cell Signaling Technology, Danvers, MA), and mouse monoclonal anti-Olig2 Ab (1:500, R&D Systems, Bio-Techne, AF2418).

Terminal deoxynucleotidyl transferase dUTP nick-end labeling (TUNEL) assay (#G3250, Promega, Madison, WI) was performed, according to the manufacturer's recommendation.

Quantitative evaluation of cerebral myelination and OLs maturation was performed on the images captured with confocal microscopy at the resolution 1024 × 1024 pixels, under magnification 20× (observed area 630 × 630 µm) projected from *Z*-stack of nine optical slices with 1 µm step. Images were transferred to Image J software, gray scaled and parameters of interest were calculated. For each mouse, three images of the EC and CC from each of the coronal sections at the bregma levels +1, +0.5, and 0 mm were analyzed. As we described previously,[8] cells ($CC1^+$, $NG2^+$) were counted in a frame 100 × 400 pixels (62 × 251 µm) applied to the images of the CC and EC obtained from the similar brain areas in relation to bregma (Figs. 1b and 2b). $CC1^+$ cells were considered mature OLs and $NG2^+$ cells were defined as undifferentiated OPCs because co-staining of NG2/Olig2 and CC1/Olig2 revealed >90% double-positive cells (Fig. 2a). The count of the cells of our interest was presented as a percentage of the total $DAPI^+$ cells count per frame. Levels of MBP were quantified based on optical density with Image J.

Detection of cellular degeneration was performed by immunostaining for cleaved caspase-3 and TUNEL (as described above). The images were captured using Zeiss AX10 microscope (Carl Zeiss Microscopy, White Plains, NY) with AxioCam ICm1 camera at the resolution 1024 × 1024 pixels and 20× magnification. Caspase-3^+ and $TUNEL^+$ cells were quantified in the areas containing at least one positive cell. Three images per each of three coronal sections taken at bregma levels +1, +0.5, and 0 mm were captured and analyzed using Image J. The data were presented as a percentage of $DAPI^+$ total cell count per field.

Western blot analysis

To exclude potential discrepancies in cerebral sampling that can affect myelin content, the entire single hemisphere was used for quantitation of MBP and CNP-ase, detected with mouse monoclonal anti-MBP Ab (1:1000, #M9758-01, United States Biological, Salem, MA) and mouse monoclonal anti-CNP-ase Ab (1:10,000, #C-5922, MilliporeSigma, St. Louis, MO). Anti-β-actin peroxidase-conjugated antibody (1:100,000, #A3854, MilliporeSigma, St. Louis, MO) was used for control of loading. Images of the blots were obtained using Fluorchem M Western Imaging System (Protein Simple, San Jose, CA) and processed with Image J software. The results were expressed as optical density ratios between the protein-specific and β-actin bands.

Electron microscopy

Randomly selected P90 mice from each group were euthanized with isoflurane, intracardially perfused with 2% glutaraldehyde and 2% PFA in 0.1 M sodium PB, pH 7.4. Brains were removed, fixed for 72 h at 4 °C. Coronal slices (~1 mm thickness) were cut and small pieces (~1 × 1 mm) containing CC and EC areas were

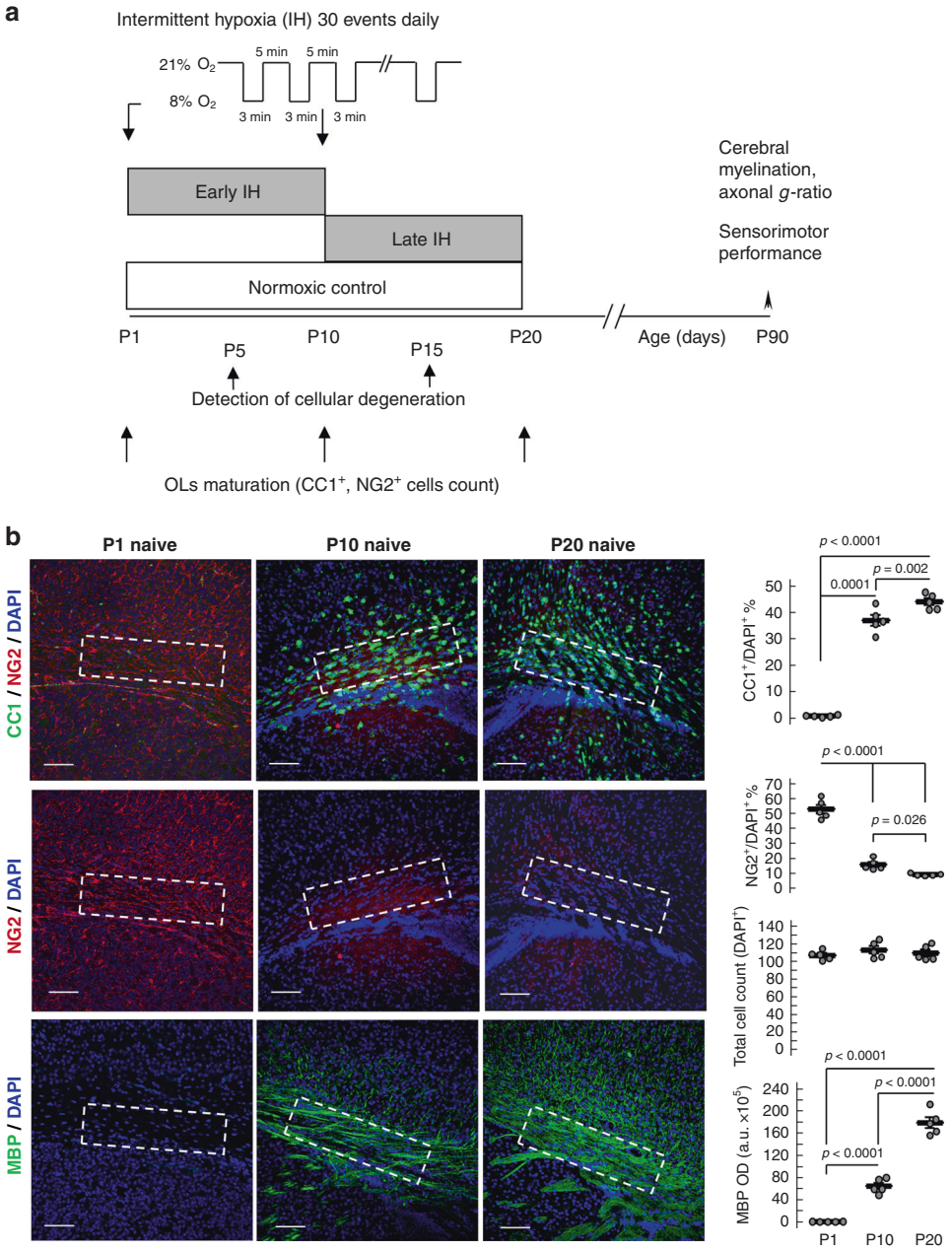

Fig. 1 Study design and primary myelination in naïve mice. a Schematic presentation of experimental design (for details, see "Methods" section). **b** Left panel: representative images of cerebral immunostaining for NG2, CC1, and MBP in neonatal naive mice at different ages. DAPI is a marker of cellularity. Dashed outlined boxes indicate the areas selected for quantification analysis, scale bar = 100 µm. Right panel: developmental changes in cellular densities ($NG2^+$ and $CC1^+$) and levels of MBP in neonatal naive mice. For cellular density, data are present as a ratio to the total number of cells ($DAPI^+$) in %. Levels of MBP are present according to OD in arbitrary units. One-way analysis of variance (ANOVA) with Fisher's post hoc test. Values are means ± SEM of five animals in each group.

dissectedout, postfixed in 2% OsO_4 in PB for 2 h at 4 °C, dehydrated with alcohol and propylene oxide, and embedded in Epon-Araldite (Electron Microscopy Sciences, Hatfield, PA). Semi-thin sections were stained with toluidine blue; areas of interest were identified under the upright microscope for the blocks trimming. Ultrathin sections were stained with uranyl acetate and lead citrate, and examined using JEOL 100 S electron microscope (JEOL, Peabody, MA) equipped with a Hamamatsu ORCA HR camera. The axonal myelination was evaluated by the calculation of the *g*-ratio: ratio of the inner axon diameter to the entire diameter of the axon with myelin sheath, as we described previously.[7] Axons with diameters <300 nm were not analyzed. At least, six images per animal captured at 20 k magnification were used for quantification. A minimum of 50 axons per animal were analyzed.

Assessment of sensorimotor performance

Sensorimotor performance was tested in P85–86 mice using three tests; wire-holding, beam-crossing, and accelerating rotarod tests, as we described.[7] The wire test was conducted using a wire 0.5 mm in diameter and 0.5 m in length, which was suspended 1.5 m above a padded surface. The time each mouse was able to hang without falling was recorded. To prevent escaping, each end of the wire was attached to claw-unfriendly plastic walls. Each mouse was given two probe trials (one a day) with no training trial, and the mean value was used for analysis. The beam test was used to evaluate

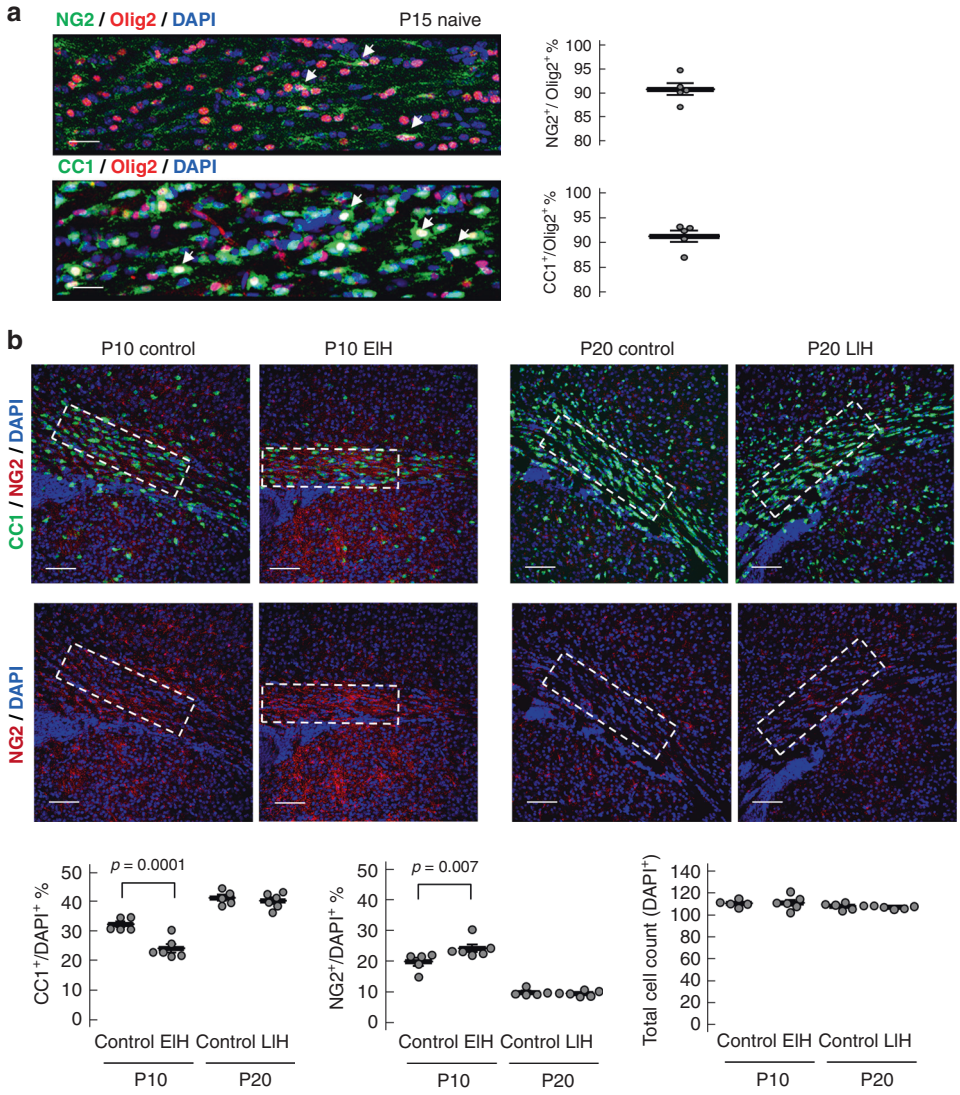

Fig. 2 Oligodendrocytes maturation during early and late IH. a Representative images of external capsule with $CC1^+$ and $NG2^+$ cells co-stained for Olig2 (indicated by white arrows) in neonatal naive P15 mice ($n = 5$) with statistical analysis for the count of double-positive cells as a % per total either NG2 positive cells or CC1-positive cells. DAPI is a marker of cellularity. Scale bar = 30 µm. **b** Representative images of $CC1^+$ and $NG2^+$ cells in neonatal control, early exposure (EIH) and late exposure (LIH) to intermittent hypoxemia mice with statistical analysis of cell count. Dashed outlined boxes indicate the areas for quantification analysis. Data are present as a ratio of the number of positive cells to the total cell count ($DAPI^+$) in %. Scale bar = 100 µm. Student *t* test. Values are as mean ± SEM of five to six animals in each group.

challenged locomotion and coordination. Adult mice were placed at the end of a round ∅17.5 mm and 1 m long beam. The time required to traverse the beam was recorded. The allotted time was 60 s. To promote beam traversing, the mouse was placed at the end of the beam attached to a claw-unfriendly wall, while a safety platform was positioned at the opposite end of the beam. Following one practice run, two probe trials were offered 10 min apart. The mean value of probe trials was used for analysis. An accelerating rotarod test was performed with minor modification. Mice were placed on an accelerating (from 16 to 32 r.p.m.) rotarod (Med Associates, St. Albans, VT). The time that each mouse was able to run on the rod was recorded. The time recording was stopped if the mouse fell from the rotarod or rotated twice around the rod without running. Each mouse was given two probe trials (one a day) with no training.

Statistical analysis

All data were presented as mean ± SEM. One-way analysis of variance (ANOVA) with Fisher's post hoc tests was performed for comparisons between multiple groups. Student *t* test was used to analyze differences between the two groups. A difference was considered significant, if $p < 0.05$.

RESULTS

Primary white matter myelination peaks during the initial days of life and is sensitive to sublethal IH

At P1, the brains of naive mice nearly completely lacked myelin, contained few mature OLs ($CC1^+$ cells), and abundance of OPCs ($NG2^+$ cells) in the areas corresponding to the CC and EC (Fig. 1b). Over the initial 10 days of life, the density of mature OLs and the extent of cerebral myelination, defined by MBP immunopositivity in CC and EC, increased dramatically and significantly surpassed those at P1 (Fig. 1b). In contrast, during the same period, the number of OPCs (NG2) has significantly decreased (Fig. 1b), indicating the OPCs maturation spurt into myelin-producing cells (CC1). Over the next ten postnatal days, naive P20 mice exhibited a significant elevation of MBP expression in their CC and EC compared to P10 mice (Fig. 1b), the density of $NG2^+$ cells

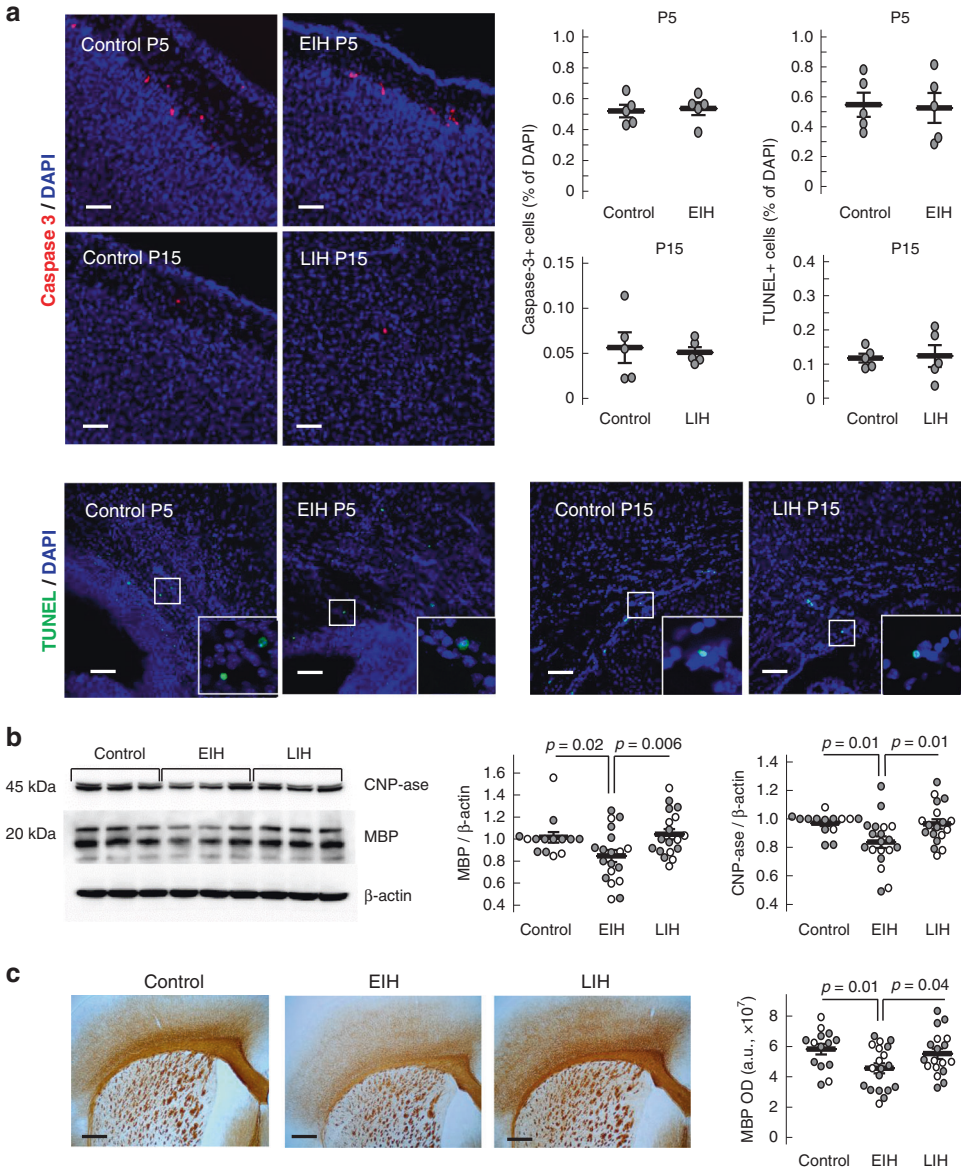

Fig. 3 Cellular death and extent of myelination. a Representative images of the cortex stained for activated caspase-3 and external capsule stained for TUNEL with statistical analysis of cells count. Scale bar = 100 µm. Data are present as a ratio of the number of positive cells to the total cell count ($DAPI^+$) in %. Student *t* test. Values are means ± SEM of five animals in each group. **B** Western blot analysis of MBP and CNP-ase content in the entire hemisphere in adult control ($n = 14$), early exposure to intermittent hypoxemia (EIH; $n = 19$) and late exposure to intermittent hypoxemia (LIH; $n = 18$) mice. White circles—males, gray circles—females. **C** Immunostaining for MBP (brown) in areas of corpus callosum, external capsule with adjacent cortex, and striatum in adult control ($n = 14$), EIH ($n = 19$), and LIH ($n = 18$) mice. White circles—males, gray circles—females. Expression of MBP in each group is present according to OD in arbitrary units. Scale bar = 500 µm. One-way ANOVA with Fisher's post hoc test. Values are means ± SEM. Analysis of the data controlled by sex is described in the "Results" section.

continued to decrease and $CC1^+$ cells count continued to increase (Fig. 1b). Of note, compared to P1 mice, in P10 naive neonatal mice, the density of mature OLs exhibited a 48.4-fold increase and only a 1.2-fold increase in P20 naive mice compared to P10 naive mice. MBP immunoreactivity has also increased drastically (164.1-fold) in P10 naive animals compared to P1 mice. On the other hand, in P20 mice, the MBP level raised only by 2.8-fold compared to that in P10 littermates (Fig. 1b). These data strongly suggest that the most intense OLs maturation and primary myelination occur during the initial 10 days of life. The total amount of cells defined with DAPI staining did not differ significantly between P1, P10, and P20 (Fig. 1b). Co-immunostaining of CC1 and NG2 cells for Olig2 reactivity demonstrated that, at P15 > 90% of these types of cells belong to the OL lineage (Fig. 2a).

Exposure to EIH significantly decreased the density of mature OLs in the white matter compared to control normoxic P10 littermates. This was coupled with a significantly greater density of OPCs (Fig. 2b), indicating a delay in OPC differentiation. In contrast, LIH did not significantly affect OLs maturation in the WM as the density of mature OLs, and OPCs did not differ compared to control normoxic P20 littermates (Fig. 2b).

EIH and LIH did not cause cell death in the brains

Cerebral immunostaining for cleaved caspase-3 and TUNEL-positive cells revealed no difference in either of the EIH or LIH groups compared with their corresponding normoxic controls at P5 and P15, respectively (Fig. 3a). Thus, the cell-nonlethal IH stress caused defects in OPC differentiation and in primary cerebral

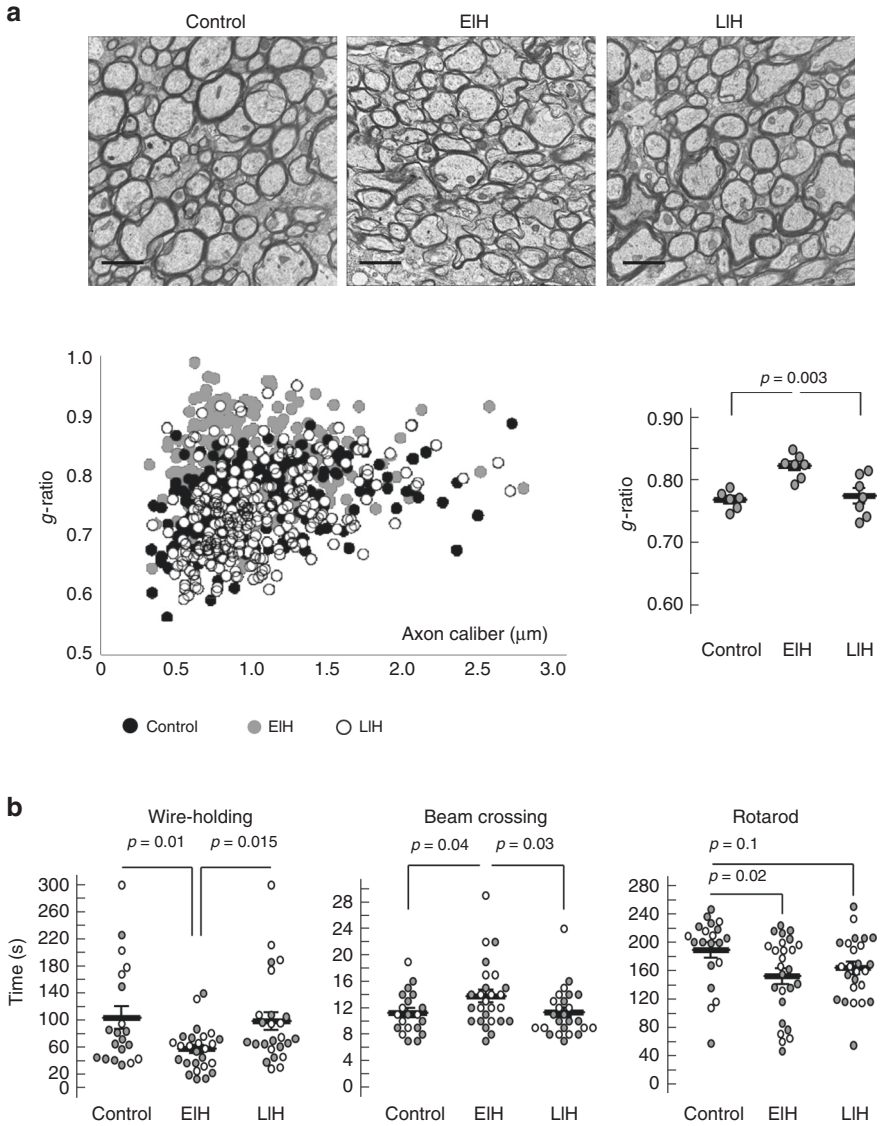

Fig. 4 Axonal myelination and sensorimotor performance. a Assessment of cerebral myelination in the corpus callosum and external capsule with electron microscopy and analysis of *g*-ratio in adult control ($n = 6$), early exposure to intermittent hypoxia (EIH; $n = 7$), and late exposure to intermittent hypoxia (LIH; $n = 7$) mice. Scale bar = 1 μm. One-way analysis of variance (ANOVA) with Fisher's post hoc test. Values are means ± SEM. **b** Sensorimotor performance in adult control ($n = 20$), EIH ($n = 26$), and LIH ($n = 25$) mice. White circles—males, gray circles—females. One-way analysis of variance (ANOVA) with Fisher' post hoc test. Values are means ± SEM. Analysis of the data controlled by sex is described in the "Results" section.

myelination only when it occurred at the initial 10 days of life. This confirms an existence of the developmental window of white matter vulnerability and dissects out cellular death-driven mechanisms in this event.

Sublethal IH causes permanent cerebral hypomyelination and the sensorimotor deficit only if applied during the initial 10 days of life Adult mice in the EIH group exhibited cerebral hypomyelination evidenced by a significant decrease in MBP and CNP-ase immunoblot expression compared to normoxic controls (Fig. 3b). Immunostaining of CC, EC, adjacent cortex, and striatum also revealed significantly decreased MBP signal only in the EIH group, compared to LIH and control groups (Fig. 3c). In contrast, there was no significant difference in cerebral myelination (MBP and CNP-ase expression) between LIH and control groups (Fig. 3b, c).

When mice were stratified by their sex, only females (gray circles, Fig. 3c) from the EIH group exhibited significantly decreased MBP expression compared to both controls ($p = 0.015$) and LIH ($p = 0.045$) counterparts. Western blot analysis controlled for sex revealed a significantly decreased CNP-ase expression only in EIH males, compared to controls ($p = 0.017$) and LIH ($p = 0.046$) counterparts, with the same tendency in females. Cerebral MBP content also demonstrated only a trend toward hypomyelination in separate groups of EIH-exposed males and females, compared to their controls and LIH groups.

Electron microscopy of CC and EC in adult mice demonstrated significantly decreased axonal myelination evaluated by *g*-ratio only in the EIH group, compared to LIH mice and normoxic controls (Fig. 4a).

Cerebral hypomyelination in mice exposed to EIH was associated with significantly poorer sensorimotor performance in wire-holding and beam-crossing tests, compared to the LIH group and normoxic littermates (Fig. 4b). The rotarod test revealed significantly worse performance in the EIH mice compared only to normoxic controls, but the difference between normoxic controls and the LIH group did not reach statistical significance (Fig. 4b).

Analysis of these data controlled for sex revealed significantly poorer wire-holding test performance only in EIH males ($p = 0.02$ vs. controls) and only a trend ($p = 0.067$), compared to LIH group. Females from EIH group also demonstrated only a trend toward poorer performance in this test. In beam-crossing and rotarod tests, separately males or females from EIH did not exhibit significantly poorer performance compared to their controls or LIH groups.

DISCUSSION

Our work demonstrates that sublethal IH stress resulted in maturational failure of OL linage cells and permanent diffuse WMI only when this stress was applied at birth and coincided with the initiation of primary WM myelination. When the same IH stress affected mice at the stage of advanced primary WM myelination, no phenotype of WMI has developed. Notably, this permanent WMI injury occurred in the absence of IH-induced cell death in the brain. Earlier, permanent diffuse WMI and failure of OLs maturation have been recapitulated without OL lineage cellular death by the exposure of newborn mice to IL-1β only during the initial 5 days of their life.[13] Taken together with these findings, our data suggest that regardless of the stress nature, IH or neuroinflammation, the WM developmental stage during the exposure defines the extent of maturation failure of viable OL and diffuse WMI. Since, we compared the effects of timing when WMI-inducing IH stress occurs during brain development, our study not only supports the existence of a window of developmental vulnerability to WMI in premature infants[4] and neonatal rodents,[11] but demonstrates that selective lethal vulnerability of immature OLs to stress is not a single mechanism driving WMI only at the certain neonatal age in IH mice. These are important and novel results because, mechanisms explaining the existence of a developmental window of vulnerability to perinatal WMI driven by hypoxia and ischemia have been linked to the selective death of OPC and pre-OLs.[3,14] In this respect, our study expands mechanistic explanation for the existence of a developmental window of vulnerability to diffuse WMI, suggesting that early maturational stage of viable OLs is vulnerable in cell-sublethal IH stress. Of note, comparative analysis of human cerebral sections with and without (control) cystic PVL lesions revealed a significantly increased density of caspase-3-positive cells only within the necrotic foci compared to controls, and compared to the remote (6 mm away) from the necrotic area, yet damaged white matter zone. These data support a contribution of OLs maturational failure to abnormal MBP patterns detected in these specimens.[15] Similarly, Verney et al. in the cerebral sections from very preterm infants have found no significant decrease in cellular density of $Olig2^+$ pre-OLs in diffuse WMI lesions, surrounding scattered necrotic foci.[16] Although these data were obtained from the brain sections with cystic PVL (cell-lethal injury), an absence of pre-OLs loss in the areas of diffuse WMI around necrotic foci suggests the co-existence of the cell-nonlethal mechanism of WMI in humans. Our animal study identifies a cerebral developmental stage when these cell-nonlethal mechanism/s cause the damage.

In naive mice, during the initial 10 days of life, we observed a dramatic increase in the density of $CC1^+$ cells and WM myelination. Over the next 10 days of life, however, these mice exhibited only modest elevation in $CC1^+$ cells content, while WM myelination remained robust. This suggests that developmentally regulated, natural deceleration in the OL maturation rate did not significantly affect myelination. These data also demonstrate that in neonatal mice, a peak of OL maturation occurs during the first 10 postnatal days. Similarly, in neonatal (P2) rats, the OL lineage predominantly contained pre-OLs,[17] which quickly, by P5, progressed into a more differentiated immature OL population.[11] Cell-nonlethal IH stress applied during this initial stage suppressed OLs differentiation, and this maturation failure was associated with permanent WM hypomyelination. In contrast, when IH of an identical severity and duration was applied after the stage of most intense OL differentiation was over, the exposure to IH did not reproduce the WMI phenotype. These data suggest that the window of vulnerability to WMI is determined by the differentiation intensity of OL precursors during postnatal stress.

To date, proposed mechanistic explanations for the existence of a developmental window of vulnerability to the WMI induced by hypoxic–ischemic and oxidative stress have been related to a fatal selective susceptibility of pre-OLs to various stresses.[18–20] The developmental stage when OPCs actively differentiate into pre-OLs has been considered the most vulnerable time point for acquiring WMI disease.[21] In rodents, this developmental stage corresponds to the initial postnatal week. Thus, when an insult (hypoxia–ischemia, intraventricular hemorrhage, and infection) coincides with this stage of OL maturation, the concept of selective susceptibility of pre-OLs to lethal stressors fairly well explains the existence of a developmental window of vulnerability to diffuse WMI. However, this concept does not explain the window of vulnerability to WMI induced by sublethal stress shown in this and other studies.[7,8,13]

It has been noted that when WMI is coupled with OLs precursors death, brain histopathology reveals significantly increased numbers of OPCs in areas of subacute injury. This has been interpreted as a compensatory response of the OPC pool to damage, in order to generate new OLs and replenish a lost OL population. However, due to unclear reasons, these newly generated OPCs fail to differentiate beyond the pre-OL stage.[2] One of the potential mechanisms behind this failure could be a dysregulation of the WNT/β-catenin pathway. This pathway is thought to be critical for myelinogenesis,[22] and when aberrant can inhibit both developmental myelination and remyelination in mice.[23] Of interest, chronic IH stress mimicking sleep apnea in humans is associated with dysregulated WNT/β-catenin signaling in the brain of mature mice.[24] Interestingly, in the model of WMI associated with systemic inflammation, cerebral WNT expression was significantly decreased in both early and late exposure to IL-1β, yet diffuse hypomyelination and OLs maturation failure were detected only after early exposure.[13] This argues against contribution of WNT/β-catenin dysregulation to an existence of the window of vulnerability in cell-nonlethal diffuse WMI. We have recently reported that cell-nonlethal IH activated cyclophilin D-dependent mitochondrial proton leak, which uncoupled mitochondrial respiration in differentiating OPCs and caused their maturation arrest in vivo and in vitro.[8] Thus, different molecular mechanisms and pathways contribute to OLs differentiation failure, including those triggered by hypoxemia.[25,26] While exact cell-nonlethal mechanisms driving differentiation failure in viable immature OLs are yet to be determined, our study frames the developmental stage when these mechanisms would be acting. It is worth discussing, that LIH was applied when developmental cerebral myelination remained robust, while OLs maturation peak has passed. Because LIH did not reproduce diffuse WMI phenotype, we reasoned that the rate of OLs differentiation rather than the intensity of primary myelination defines a vulnerability to WMI. Of interest, mature conditionally COX10 (a critical component of complex IV) knock-out mice maintained normal axonal myelination, suggesting that mature OLs are glycolytic and oxidative phosphorylation is not critical for myelination.[27]

In this study, the data stratified by a sex only partially supported the conclusion, demonstrating statistical significance in some tests and only trends in other tests for both sexes. Because our study was not powered to identify a sex-determined differences in the timing of the window of vulnerability to WMI, future research will address this important question.

In conclusion, together with reported research supporting fatal-selective sensitivity of OLs to stress, we show that IH-driven cell-

nonlethal mechanisms of OLs dysmaturation target the same narrow developmental window of vulnerability to WMI. Our work does not contradict the concept of OPC and pre-OL-selective sensitivity to lethal stress in defining this window, but offers experimental evidence that in the absence of cellular death, the timing of diffuse WMI formation does not display developmental shift and remains the same as in WMI driven by cell-lethal stress.

ACKNOWLEDGEMENTS

This work was supported by NIH grants NS099109 and in part by NS100850 (V.S.T.). Image processing for this work was performed in the Confocal and Specialized Microscopy Shared Resource of the Herbert Irving Comprehensive Cancer Center at Columbia University, supported by NIH grant P30 CA013696 (National Cancer Institute).

AUTHOR CONTRIBUTIONS

S.A.S., V.I.R., and V.S.T. made substantial contributions to conception and design. S.A.S. and Z.V.N. made substantial contributions to data acquisition. All authors contributed to the analysis and interpretation of data, drafting/revising the intellectual content. All authors approved the final version to be published.

ADDITIONAL INFORMATION

Competing interests: The authors declare no competing interests.

Publisher's note Springer Nature remains neutral with regard to jurisdictional claims in published maps and institutional affiliations.

REFERENCES

1. Wilson-Costello, D., Friedman, H., Minich, N., Fanaroff, A. & Hack, M. Improved survival rates with increased neurodevelopmental disability for extremely low birth weight infants in the 1990s. *Pediatrics* **115**, 997–1003 (2005).
2. Back, S. A. White matter injury in the preterm infant: pathology and mechanisms. *Acta Neuropathol.* **134**, 331–349 (2017).
3. Volpe, J. J., Kinney, H. C., Jensen, F. E. & Rosenberg, P. A. The developing oligodendrocyte: key cellular target in brain injury in the premature infant. *Int. J. Dev. Neurosci.* **29**, 423–440 (2011).
4. Back, S. A. et al. Late oligodendrocyte progenitors coincide with the developmental window of vulnerability for human perinatal white matter injury. *J. Neurosci.* **21**, 1302–1312 (2001).
5. Rakic, S. & Zecevic, N. Early oligodendrocyte precursor cells in the human fetal telencephalon. *Glia* **41**, 117–127 (2003).
6. Back, S. A. & Volpe, J. J. Cellular and molecular pathogenesis of periventricular white matter injury. *MRDD Res. Rev.* **3**, 96–107 (1997).
7. Juliano, C. et al. Mild intermittent hypoxemia in neonatal mice causes permanent neurofunctional deficit and white matter hypomyelination. *Exp. Neurol.* **264**, 33–42 (2015).
8. Niatsetskaya, Z. et al. Cyclophilin D–dependent oligodendrocyte mitochondrial ion leak contributes to neonatal white matter injury. *J. Clin. Investig.* **130**, 5536–5550 (2020).
9. Poets, C. F. et al. Association between intermittent hypoxemia or bradycardia and late death or disability in extremely preterm infants. *JAMA J. Am. Med. Assoc.* **314**, 595–603 (2015).
10. Di Fiore, J. M. et al. A higher incidence of intermittent hypoxemic episodes is associated with severe retinopathy of prematurity. *J. Pediatr.* **157**, 69–73 (2010).
11. Dean, J. M. et al. Strain-specific differences in perinatal rodent oligodendrocyte lineage progression and its correlation with human. *Dev. Neurosci.* **33**, 251–260 (2011).
12. Verity, A. N. & Campagnoni, A. T. Regional expression of myelin protein genes in the developing mouse brain: in situ hybridization studies. *J. Neurosci. Res.* **21**, 238–248 (1988).
13. Favrais, G. et al. Systemic inflammation disrupts the developmental program of white matter. *Ann. Neurol.* **70**, 550–565 (2011).
14. Haynes, R. L., Billiards, S. S., Borenstein, N. S., Volpe, J. J. & Kinney, H. C. Diffuse axonal injury in periventricular leukomalacia as determined by apoptotic marker fractin. *Pediatr. Res* **63**, 656–661 (2008).
15. Billiards, S. S. et al. Myelin abnormalities without oligodendrocyte loss in periventricular leukomalacia. *Brain Pathol.* **18**, 153–163 (2008).
16. Verney, C. et al. Microglial reaction in axonal crossroads is a hallmark of noncystic periventricular white matter injury in very preterm infants. *J. Neuropathol. Exp. Neurol.* **71**, 251–264 (2012).
17. Craig, A. et al. Quantitative analysis of perinatal rodent oligodendrocyte lineage progression and its correlation with human. *Exp. Neurol.* **181**, 231–240 (2003).
18. Back, S. A. et al. Selective vulnerability of late oligodendrocyte progenitors to hypoxia-ischemia. *J. Neurosci.* **22**, 455–463 (2002).
19. Fern, R. & Moller, T. Rapid ischemic cell death in immature oligodendrocytes: a fatal glutamate release feedback loop. *J. Neurosci.* **20**, 34–42 (2000).
20. Baud, O. et al. Glutathione peroxidase-catalase cooperativity is required for resistance to hydrogen peroxide by mature rat oligodendrocytes. *J. Neurosci.* **24**, 1531–1540 (2004).
21. Buser, J. et al. Timing of appearance of late oligodendrocyte progenitors coincides with enhanced susceptibility of preterm rabbit cerebral white matter to hypoxia-ischemia. *J. Cereb. Blood Flow. Metab.* **30**, 1053–1065 (2010).
22. Tawk, M. et al. Wnt/beta-catenin signaling is an essential and direct driver of myelin gene expression and myelinogenesis. *J. Neurosci.* **31**, 3729–3742 (2011).
23. Fancy, S. P. et al. Dysregulation of the Wnt pathway inhibits timely myelination and remyelination in the mammalian CNS. *Genes Dev.* **23**, 1571–1585 (2009).
24. Yue-Ying, P. et al. Altered Wnt signaling pathway in cognitive impairment caused by chronic intermittent hypoxia: focus on glycogen synthase kinase-3β and β-catenin. *Chin. Med. J.* **129**, 838–845 (2016).
25. Scafidi, J. et al. Intranasal epidermal growth factor treatment rescues neonatal brain injury. *Nature* **506**, 230–234 (2014).
26. Van Steenwinckel, J. et al. Decreased microglial Wnt/β-catenin signalling drives microglial pro-inflammatory activation in the developing brain. *Brain* **142**, 3806–3833 (2019).
27. Fünfschilling, U. et al. Glycolytic oligodendrocytes maintain myelin and long-term axonal integrity. *Nature* **485**, 517–521 (2012).